Translational Oncology 14 (2021) 100886

Contents lists available at ScienceDirect

Translational Oncology

journal homepage: www.elsevier.com/locate/tranon

5-Aminolevulinic acid for fluorescence-guided surgery in pancreatic cancer: Cellular transport and fluorescence quantification studies

P.L. Labib [a,*], E. Yaghini [b], B.R. Davidson [b], A.J. MacRobert [b], S.P. Pereira [a]

[a] UCL Institute for Liver & Digestive Health, University College London, Royal Free Campus, Rowland Hill Street, London NW3 2PF, United Kingdom of Great Britain and Northern Ireland
[b] UCL Division of Surgery & Interventional Science, University College London, Royal Free Campus, Rowland Hill Street, London NW3 2PF, United Kingdom of Great Britain and Northern Ireland

ARTICLE INFO

Article history:
Received 21 August 2020
Received in revised form 10 September 2020
Accepted 11 September 2020

ABSTRACT

5-Aminolevulinic acid (ALA) is a potential contrast agent for fluorescence-guided surgery in pancreatic ductal adenocarcinoma (PDAC). However, factors influencing ALA uptake in PDAC have not been adequately assessed. We investigated ALA-induced porphyrin fluorescence in PDAC cell lines CFPAC-1 and PANC-1 and pancreatic ductal cell line H6c7 following incubation with 0.25–1.0 mM ALA for 4–48 h. Fluorescence was assessed qualitatively by microscopy and quantitatively by plate reader and flow cytometry. Haem biosynthesis enzymes and transporters were measured by quantitative polymerase chain reaction (qPCR). CFPAC-1 cells exhibited intense fluorescence under microscopy at low concentrations whereas PANC-1 cells and pancreatic ductal cell line H6c7 showed much lower fluorescence. Quantitative fluorescence studies demonstrated fluorescence saturation in the two PDAC cell lines at 0.5 mM ALA, whereas H6c7 cells showed increasing fluorescence with increasing ALA. Based on the PDAC:H6c7 fluorescence ratio studies, lower ALA concentrations provide better contrast between PDAC and benign pancreatic cells. Studies with qPCR showed upregulation of ALA influx transporter PEPT1 in CFPAC-1, whereas PANC-1 upregulated the efflux transporter ABCG2. We conclude that PEPT1 and ABCG2 expression may be key contributory factors for variability in ALA-induced fluorescence in PDAC.

Introduction

Due to the late onset of specific symptoms, most patients with pancreatic ductal adenocarcinoma (PDAC) are diagnosed with inoperable disease and only 13–22% will undergo curative-intent resection [1]. Even in patients selected for surgery, the majority will develop cancer recurrence. One major factor influencing this is the difficulty in achieving clear surgical resection margins. A recent systematic review of patients undergoing pancreaticoduodenectomy for PDAC (n = 3815) found that 47–92% of patients developed recurrence [2]. In the studies reporting on the site of recurrence (n = 1713), 12% of patients developed local recurrence at the resection site with no distant metastases. This suggests that in this cohort, small volume residual disease was present in the surgical field at the time of surgery but was not detected. Identifying residual tumour intraoperatively could allow surgeons to extend the resection margin (if technically possible) or help select those patients who may benefit from additional intraoperative or post-operative therapies, aiming to reduce local recurrent disease and improve survival.

Fluorescence-guided surgery (FGS) uses contrast agents that accumulate within cancers to provide intraoperative real-time enhanced tumour visualisation [3]. The signal-to-noise ratio (SNR, or tumour-to-background ratio in this context) quantifies the extent to which tumour fluoresces more than surrounding non-neoplastic tissue, and a high ratio is desirable. A SNR > 5 is often applied as a minimum desirable SNR for effective FGS [4]. FGS is attracting increasing interest in surgical oncology using a range of contrast agents [5]. However, a suitable contrast agent for FGS in PDAC has not yet been established.

5-Aminolevulinic acid (ALA) is a unique contrast agent since it acts as a pro-drug precursor of protoporphyrin IX (PpIX), a fluorescent porphyrin that is the penultimate molecule in the haem biosynthesis pathway (Fig. 1) [6,7]. ALA usually enters cells via peptide transporters PEPT1 or PEPT2 [8,9]. A large influx of exogenous ALA results in PpIX accumulation, causing cells to fluoresce red when excited with violet light. ALA has regulatory approval and is used in FGS for malignant gliomas [10].

Studies on ALA FGS in PDAC have focused on staging laparoscopy, aiming to increase detection of occult metastases to prevent unnecessary laparotomy. Orth et al. performed standard and ALA fluorescence laparoscopy (FL) in 12 patients with PDAC [11]. FL increased the number of detected peritoneal lesions (19 vs. 32 biopsies) but six lesions (19%) were false positives secondary to inflammation. Zöpf et al. (2005) performed a

* Corresponding author.
E-mail addresses: peter.labib@nhs.net, (P.L. Labib), elnaz.yaghini@ucl.ac.uk, (E. Yaghini), b.davidson@ucl.ac.uk, (B.R. Davidson), a.macrobert@ucl.ac.uk, (A.J. MacRobert), stephen.pereira@ucl.ac.uk. (S.P. Pereira).

http://dx.doi.org/10.1016/j.tranon.2020.100886

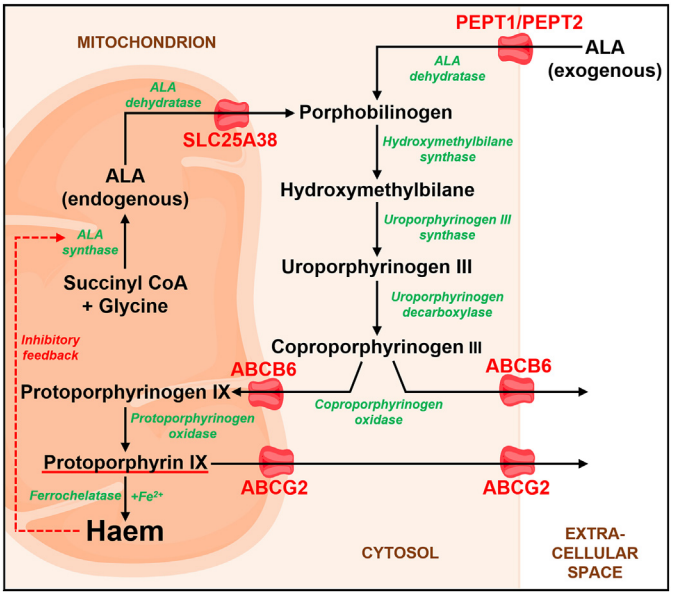

Fig. 1. The haem biosynthesis pathway. Endogenous aminolevulinic acid (ALA) is synthesised in the mitochondria and acts as an early substrate for the haem biosynthesis pathway. The penultimate molecule protoporphyrin IX (PpIX) displays bright red fluorescence when excited by blue/violet light. Exogenous ALA preferentially accumulates in neoplastic cells leading to an accumulation of PpIX that can be exploited for biophotonic diagnostics. Image constructed using icons from Servier Medical Art (licensed under CC BY 3.0). (For interpretation of the references to colour in this figure legend, the reader is referred to the web version of this article.)

similar study in patients undergoing FL for various malignancies ($n = 30$) [12]. Of the 12 PDAC patients, four had metastases and three had their metastases detected by standard and ALA FL. The fourth had a posterior liver metastasis not detected with either modality due to its location. Yonemura et al. performed ALA FL to identify peritoneal metastases in patients undergoing cytoreductive surgery, five of whom had PDAC [13]. The smallest metastasis detected by FL was 0.5 mm, with four of the five patients with PDAC demonstrating fluorescence. Harada et al. performed ALA FL in 34 patients with PDAC [14]. Nine (26%) had peritoneal nodules identified in white light, four of which fluoresced under violet light. Frozen section confirmed the four fluorescent nodules to be PDAC and the five non-fluorescent nodules to be benign. However, ALA FGS did not identify any new nodules compared to white light.

Based on these studies, ALA FGS in PDAC requires improvement and a better understanding of ALA uptake by normal pancreas and PDAC is needed. This study investigated variability in ALA uptake and metabolism in two PDAC cell lines and a pancreatic ductal cell line representing normal pancreas. Fluorescence was quantified to determine the optimal ALA concentration and incubation time for the highest SNRs. Expression of haem biosynthesis enzymes and transporters was determined to assess whether these contribute to variability in ALA-induced PpIX fluorescence in PDAC.

Materials and methods

Cell lines and culture

CFPAC-1 (ECACC, UK) was derived from a liver metastasis of a well-differentiated PDAC in a 26-year-old male [15]. PANC-1 (RIKEN BRC, Japan) was derived from a poorly-differentiated PDAC in a 56-year-old female [15]. H6c7 (Kerafast, USA) is an immortalised pancreatic ductal cell line. Derived from a 51-year-old female who underwent pancreaticoduodenectomy but whose histology showed no evidence of malignancy, it has a near-normal phenotype and genotype and is considered to represent normal pancreatic ductal cells [16,17]. CFPAC-1 was cultured in Iscove's modified Dulbecco's medium with L-glutamine, HEPES buffer (Gibco™) and 10% foetal bovine serum (FBS) (Gibco™). PANC-1 was cultured in Dulbecco's modified Eagle's medium with glucose, L-glutamine (Lonza®) and FBS. H6c7 was cultured in Keratinocyte FBS-free media with L-glutamine, epidermal growth factor and bovine pituitary extract (Gibco™) with 1% antibiotic/antimycotic (Gibco™). Cells were cultured in 75 cm^2 tissue culture flasks in a humidified incubator at 37.0 °C with 5% CO_2 and passaged when ~80% confluent.

Fluorescence microscopy

CFPAC-1, PANC-1 and H6c7 were seeded on day 1 (7500, 7500 and 9000 cells per dish respectively) and microscopy performed on day 3. These seeding densities were selected so that cell confluence was comparable between cell lines at the time of microscopy (~70%). Prior to imaging, cells were incubated for 4 or 24 h with either FBS-free cell culture medium (CCM) or 0.25/0.5/0.75/1.0 mM ALA (Sigma-Aldrich®) in FBS-free CCM. A maximum concentration of 1.0 mM was chosen based on published data on the colorectal cancer cell line WiDr demonstrating that ALA concentrations >1.0 mM do not result in further PpIX formation [18]. FBS-free CCM was used as FBS proteins cause efflux of intracellular ALA-induced PpIX [19]. After incubation, cells were fixed in 4% formaldehyde and washed in phosphate buffered saline (PBS) prior to imaging on an Olympus® BX63 fluorescence microscope (excitation/emission 545/620 nm, 10× magnification, 10 s exposure time).

Quantitative fluorescence measurements

CFPAC-1, PANC-1 and H6c7 were seeded into 96 well plates on day 1 (3000, 4000 and 8000 cells per well respectively) and had fluorescence measured on day 4 using a Tecan® Infinite® 200 PRO plate reader (excitation/emission 420/635 nm). These seeding densities were selected so that cell confluence was comparable between all cell lines at the time of measurement (~80%). Prior to measurement, cells were incubated with either FBS-free CCM (control) or 0.25/0.5/0.75/1.0 mM ALA in FBS-free CCM for 4, 8, 24 or 48 h and washed with PBS.

Observed differences between cell lines using a plate reader may be secondary to variations in cell numbers, cell size or growth rates in each well. To address this, flow cytometry using fluorescence-activated cell sorting determined fluorescence values for individual cells. A set number of cells (events) were analysed to calculate the median per-cell fluorescence. 1×10^6 cells were seeded onto 25 cm^2 tissue culture flasks on day 1 and flow cytometry performed on day 3 following 4 or 24 h incubation with FBS-free CCM (control) or 0.25/0.5/0.75/1.0 mM ALA in FBS-free CCM (excitation 405 nm, emission 600–620 nm). Samples were trypsinised, washed and centrifuged before being stained with a viability dye to identify live cells (Invitrogen™ eBioscience™ eFluor™ 450, excitation/emission 405/450 nm). This dye was selected as its narrow emission peak at 450 nm does not overlay the emission peak of PpIX at 635 nm. Samples were analysed on a BD LSRFortessa™ 5 L SORP cell analyser until 30,000 events were recorded. Live cells were gated and median per-cell fluorescence calculated using FlowJo v10.6. Compensation was applied to deduct any red fluorescence emission attributable to the viability dye.

Toxicity assessment

Cell metabolic activity was assessed using the Methyl Thiazolyl Tetrazolium (MTT) assay. CFPAC-1, PANC-1 and H6c7 were seeded on day 1 (3000, 4000 and 8000 cells per well respectively) and absorbance at 570 nm read on the plate reader on day 4 following 24 or 48 h exposure to FBS-free CCM (control) or 0.25/0.5/0.75/1.0 mM ALA in FBS-free CCM. Cells were incubated with MTT for 3 h prior to reading and were shielded from light to assess toxicity from ALA exposure rather than ALA-induced photodynamic therapy.

Quantitative polymerase chain reaction (qPCR)

Quantitative PCR was performed to investigate the effect of ALA on mRNA expression of haem biosynthesis enzymes and transporters [6,7]. 1×10^6 cells were seeded on 10 cm petri dishes on day 1. On day 2, the media was changed to FBS-free CCM (control) or 0.5 mM ALA in FBS-free CCM. On day 3 (24 h ALA exposure), RNA was extracted (RNeasy minikit, QIAGEN®) as per manufacturer's instructions and complementary DNA (cDNA) synthesised using High Capacity cDNA Reverse Transcription (RT) Kit (Applied Biosystems®). To synthesise cDNA, samples were diluted with RNA-free water to a concentration of 100 ng μl^{-1}, combined with Master Mix prepared to manufacturer instructions and reverse transcription performed using a Q-Cycler II thermal cycler (Quanta Biotech Ltd.). qPCR was performed using an ABI 7500 Fast Real time PCR System (Applied Biosystems®) and custom TaqMan™ array plates. Probes targeted the following mRNA sequences:

- Enzymes: ALA synthase, ALA dehydratase, hydroxymethylbilane synthase, uroporphyrinogen III synthase, uroporphyrinogen III decarboxylase, coproporphyrinogen oxidase, protoporphyrinogen oxidase, ferrochelatase.
- Transporters: PEPT1, PEPT2, ABCB6, ABCG2, SLC25A38.

Relative mRNA expression was normalised to housekeeping gene HPRT1.

Statistics and data processing

Comparison of groups used one-way analysis of variance (ANOVA) with $p < 0.05$ being considered statistically significant. Post-hoc analyses used the Dunn-Bonferroni correction to reduce the risk of type I error from multiple *t*-tests ($p < 0.005$ being considered statistically significant). Similarly, comparison of mRNA expression changes following ALA exposure had significance set at a $p < 0.01$ to reduce the risk of type I error. Plate reader, flow cytometry, toxicity and qPCR experiments were performed in triplicate. Images were processed using ImageJ v.1.5 and plate reader and qPCR data using Excel 2013. Statistics were performed on IBM® SPSS® Statistics 24 and graphs constructed using GraphPad Prism 8.

Results

Fluorescence microscopy

CFPAC-1 exhibited strong PpIX fluorescence at each ALA concentration after 4 or 24 h incubation (Fig. 2). Characteristic extranuclear fluorescence distribution was observed in all cells, and cells appeared healthy demonstrating the normal lattice growth pattern typical of CFPAC-1. PANC-1 demonstrated no discernible PpIX fluorescence at any investigated ALA concentration after 4 h incubation. After 24 h, weak fluorescence was detectable from 0.5 mM ALA onwards. H6c7 demonstrated increasing

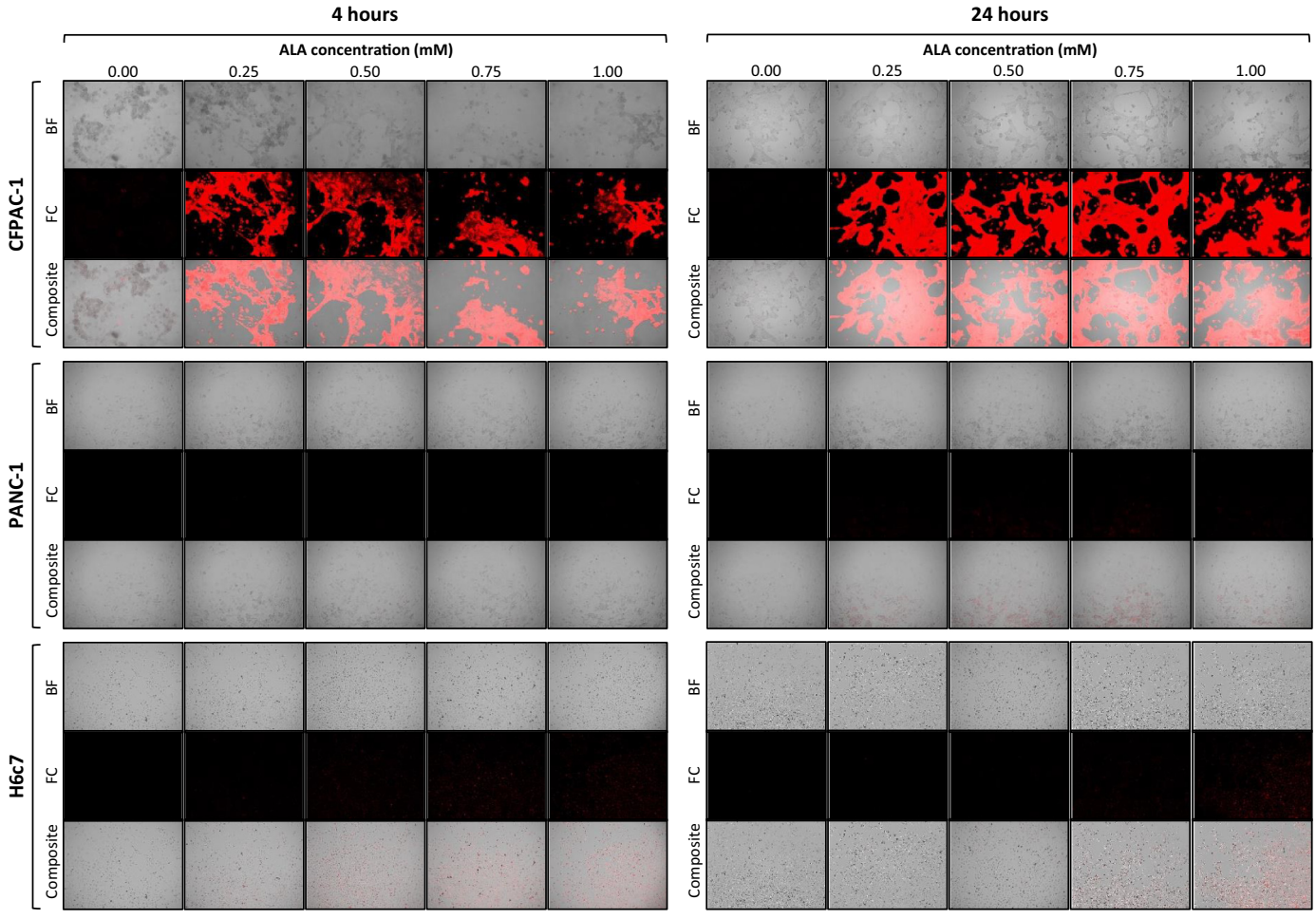

Fig. 2. Fluorescence microscopy of pancreatic cancer cell lines CFPAC-1 and PANC-1 and pancreatic ductal cell line H6c7 following 4 or 24 h incubation with increasing doses of aminolevulinic acid. CFPAC-1 demonstrated bright ALA-induced fluorescence at all investigated ALA concentrations after 4 or 24 h incubation with ALA. In contrast, PANC-1 showed minimal ALA-induced fluorescence (strongest signal at higher doses of ALA after 24 h exposure). The control cell line H6c7, although showing little fluorescence at lower concentrations, demonstrated increasing fluorescence at higher concentration at both 4 and 24 h. Abbreviations: BF = bright field, FC = fluorescence channel (emission 620 nm), ALA = 5-aminolevulinic acid. 10× magnification, individual image size 877 × 661 μm.

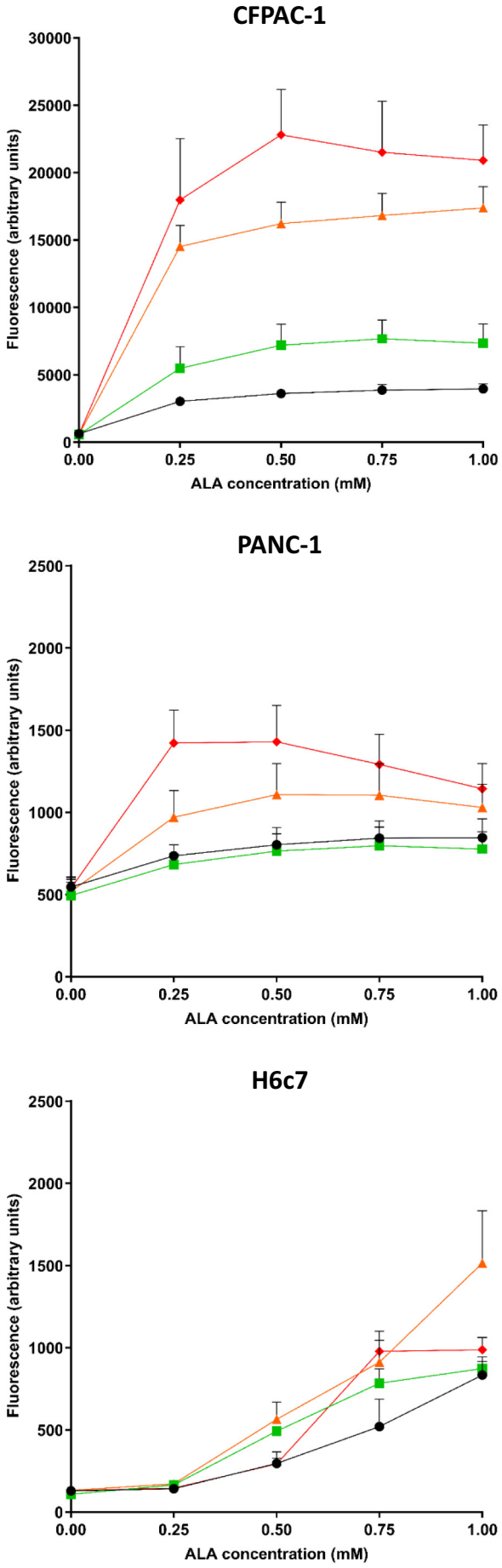

fluorescence from 0.5 mM after 4 h incubation and from 0.75 mM after 24 h incubation.

Quantitative fluorescence

Plate reader data showed that compared to CFPAC-1 in CCM, incubation with ALA resulted in significantly increased mean fluorescence at all investigated time points and ALA concentrations (one-way ANOVA $p < 0.0001$) (Fig. 3). Post-hoc analysis showed that a threshold was reached where further increases in ALA concentration did not cause significantly higher fluorescence (0.75 mM at 4 h and 0.5 mM after 8, 24 or 48 h). PANC-1 also showed a significant increase in mean fluorescence after ALA exposure compared to PANC-1 in CCM (one-way ANOVA $p < 0.0001$), although the increase was small compared to CFPAC-1. Post-hoc analysis showed no further significant fluorescence increase at ALA concentrations >0.5 mM at all four time points. H6c7 incubated with ALA also showed significantly increased mean fluorescence compared to H6c7 in CCM at all investigated time points (one-way ANOVA $p < 0.0001$). Post-hoc analysis showed that whilst there was no significant difference in mean fluorescence between cells in CCM and cells incubated with 0.25 mM ALA, there was a significant increase in fluorescence between control cells and cells incubated with 0.5, 0.75 or 1.0 mM ALA.

Flow cytometry results correlated well with plate reader data. CFPAC-1 with ALA had a significantly higher median per-cell fluorescence at all investigated time points and concentrations compared to CFPAC-1 in CCM (one-way ANOVA $p < 0.0001$) (Fig. 4). Post-hoc analysis showed no further significant fluorescence increase with ALA concentrations >0.25 mM after 4 or 24 h. After 4 h, there was no significant increase in median fluorescence in PANC-1 with ALA compared to PANC-1 in CCM (one-way ANOVA $p = 0.119$). However, PANC-1 demonstrated significantly increased median fluorescence after 24 h (one-way ANOVA $p < 0.0001$). Post-hoc analysis showed a significant increase between PANC-1 in CCM and PANC-1 with 0.25 mM ALA, but no further significant fluorescence increase with ALA concentrations >0.25 mM. H6c7 had a significantly increased median per-cell fluorescence after 4 and 24 h incubation with ALA compared to H6c7 in CCM (one-way ANOVA $p < 0.0001$ and $p = 0.001$ respectively). Post-hoc analysis showed that after 4 h, there was no significant difference between H6c7 in CCM and H6c7 with 0.25 mM ALA but a significant median fluorescence increase from 0.5 mM ALA onwards. After 24 h incubation, there was no significant difference between H6c7 in CCM and H6c7 up to 0.5 mM ALA but a significant median fluorescence increase from 0.75 mM ALA onwards.

Signal-to-noise ratios

To calculate SNRs, the mean fluorescence of CFPAC-1 and PANC-1 from the flow cytometry experiments were divided by the mean fluorescence of H6c7 at all investigated time points and ALA concentrations (Tables 1 and 2). In both cell lines, SNRs were higher after 24 h compared to 4 h. Increasing the ALA concentration reduced the SNR as H6c7 had increasing fluorescence at higher ALA concentrations. Therefore, the best ratios were seen at 24 h with lower ALA concentrations. SNRs in PANC-1 were much lower than CFPAC-1 due to the poor uptake of ALA in PANC-1 and increasing

Fig. 3. Quantitative fluorescence measurements of pancreatic cancer cell lines CFPAC-1 and PANC-1 and pancreatic ductal cell line H6c7 following 4, 8, 24 or 48 h incubation with increasing doses of aminolevulinic acid using a plate reader. Black (circle) = 4 h, green (square) = 8 h, orange (triangle) = 24 h, diamond (red) = 48 h. Increasing incubation time with ALA resulted in significant increased fluorescence in CFPAC-1 at all observed concentrations. In contrast, PANC-1 only demonstrated a moderate increase in red fluorescence. The pancreatic ductal cell line H6c7 also showed very little increase in red fluorescence, although reached a fluorescence similar to PANC-1 at higher ALA concentrations (0.75–1.00 mM). Please note different y axis scale for CFPAC-1. (For interpretation of the references to colour in this figure legend, the reader is referred to the web version of this article.)

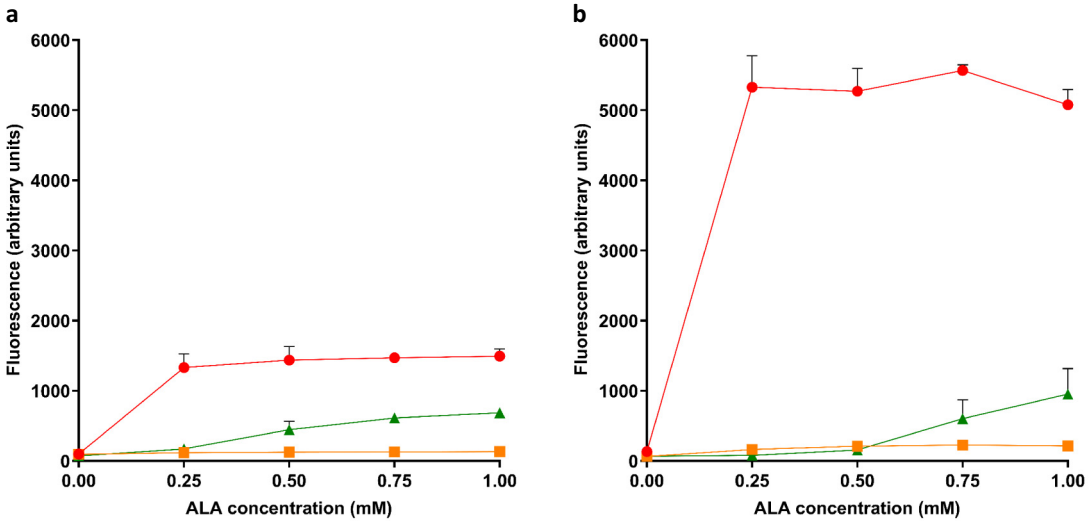

Fig. 4. Median per-cell fluorescence measurements in pancreatic cancer cell lines CFPAC-1 and PANC-1 and pancreatic ductal cell line H6c7 following 4 or 24 h incubation with increasing doses of aminolevulinic acid using flow cytometry. a = 4 h, b = 24 h. Red (circle) = CFPAC-1, orange (square) = PANC-1, green (triangle) = H6c7. ALA = aminolevulinic acid. CFPAC-1 demonstrated a significant increase in median per-cell fluorescence after 4 or 24 h incubation with 0.25 mM ALA, with no further significant increase achieved by increasing ALA concentrations. PANC-1 did not have a statistically significant increase in fluorescence at any ALA concentration after 4 h, but had a significant increase after 24 h exposure that plateaued at 0.50 mM. At both time points, H6c7 showed gradually increasing fluorescence that was least marked at the lowest investigated ALA concentration (0.25 mM). (For interpretation of the references to colour in this figure legend, the reader is referred to the web version of this article.)

ALA uptake in Hc67 at higher concentrations. No experimental condition in PANC-1 achieved a SNR >5.0.

Toxicity

PANC-1 and H6c7 showed no significant reduction in cell viability on MTT assay (Fig. 5). CFPAC-1 showed a significant reduction in metabolic activity at all investigated ALA concentrations after 24 or 48 h incubation (one-way ANOVA <0.001 for both time points).

Cell metabolic activity was ~60% after 24 h and ~50% after 48 h incubation at all investigated ALA concentrations.

Quantitative real-time polymerase chain reaction (qPCR)

Pre-ALA exposure, CFPAC-1 expressed PEPT1 and PANC-1 expressed PEPT2 (Fig. 6). ALA synthase and ABCB6 were expressed in all three cell lines, as well as low-level expression of porphyrin efflux transporter ABCG2.

Post-ALA exposure, CFPAC-1 significantly downregulated PEPT1 and ALA synthase and significantly upregulated coproporphyrinogen III efflux transporter ABCB6. PANC-1 also significantly upregulated ABCG2. H6c7 demonstrated significant upregulation of transporters PEPT2, SLC25A38, ABCB6 and ABCG2 and enzymes uroporphyrinogen decarboxylase, coproporphyrinogen oxidase, protoporphyrinogen oxidase and ferrochelatase. ALA synthase was also significantly downregulated.

Discussion

Several studies have suggested that ALA can be used as a contrast agent in FGS for PDAC [11–14]. However, they have shown only limited clinical benefit with current ALA dosing and detection methods. Mechanistic insights into ALA-induced fluorescence in PDAC are needed to identify reasons for variable uptake and mechanisms for optimising ALA FGS. To our knowledge, this is the first study that quantifies ALA-induced fluorescence in PDAC and correlates this with a detailed assessment of haem biosynthetic transporters and enzymes.

CFPAC-1 demonstrated intense red fluorescence even at the lowest investigated ALA concentration (Fig. 2) and was even visible to the naked eye without magnification. Consistent with Harada et al. [14], this suggests that small volume cancer deposits can be detected by direct vision following ALA uptake. However, ALA did not induce discernible fluorescence in PANC-1 despite high ALA concentrations. Similar to ALA studies on the colorectal cancer cell line WiDr, this implies that the limiting factor for PpIX accumulation in PANC-1 is not the extracellular availability of ALA [18]. H6c7 only exhibited fluorescence at higher ALA concentrations, suggesting that mechanisms preventing PpIX accumulation in benign pancreatic ductal cells are overcome at high ALA concentrations.

Quantitative fluorescence showed that fluorescence increased significantly in CFPAC-1 and PANC-1 using 0.25 mM ALA with minimal further fluorescence increases seen at higher concentrations (Figs. 3 and 4). H6c7 showed negligible fluorescence at 0.25 mM ALA but increasing fluorescence with higher ALA concentrations. As SNRs are calculated by dividing

Table 1
CFPAC-1:H6c7 and PANC-1:H6c7 signal-to-noise ratios. CFPAC-1:H6c7 (left-hand side) and PANC-1:H6c7 (right-hand side) signal-to-noise ratios (SNRs). SNRs were calculated by dividing the mean fluorescence of CFPAC-1 and PANC-1 (cancer cell line) by the mean fluorescence of H6c7 (representing normal pancreas). Underlined value = SNR ≥ 5.0. For both cell lines the highest SNRs were seen at longer incubation times with lower ALA concentrations.

CFPAC-1 Signal-to-Noise Ratio (SNR)		ALA concentration (mM)			
		0.25	0.50	0.75	1.00
Incubation time (h)	4	7.8	3.2	2.4	2.2
	24	66.5	33.8	9.2	5.3

Table 2
CFPAC-1:H6c7 and PANC-1:H6c7 signal-to-noise ratios. CFPAC-1:H6c7 (left-hand side) and PANC-1:H6c7 (right-hand side) signal-to-noise ratios (SNRs). SNRs were calculated by dividing the mean fluorescence of CFPAC-1 and PANC-1 (cancer cell line) by the mean fluorescence of H6c7 (representing normal pancreas). Underlined value = SNR ≥ 5.0. For both cell lines the highest SNRs were seen at longer incubation times with lower ALA concentrations.

PANC-1 Signal-to-Noise Ratio (SNR)		ALA concentration (mM)			
		0.25	0.50	0.75	1.00
Incubation time (h)	4	0.7	0.3	0.2	0.2
	24	2.0	1.4	0.4	0.2

cancer cell fluorescence by control cell fluorescence, the SNRs were highest at the lowest investigated ALA concentration (Tables 1 and 2). These data are consistent with research in breast cancer cell lines demonstrating higher SNRs at lower ALA concentrations [20]. However, SNRs calculated using cell lines do not represent a complex pancreatic tumour microenvironment.

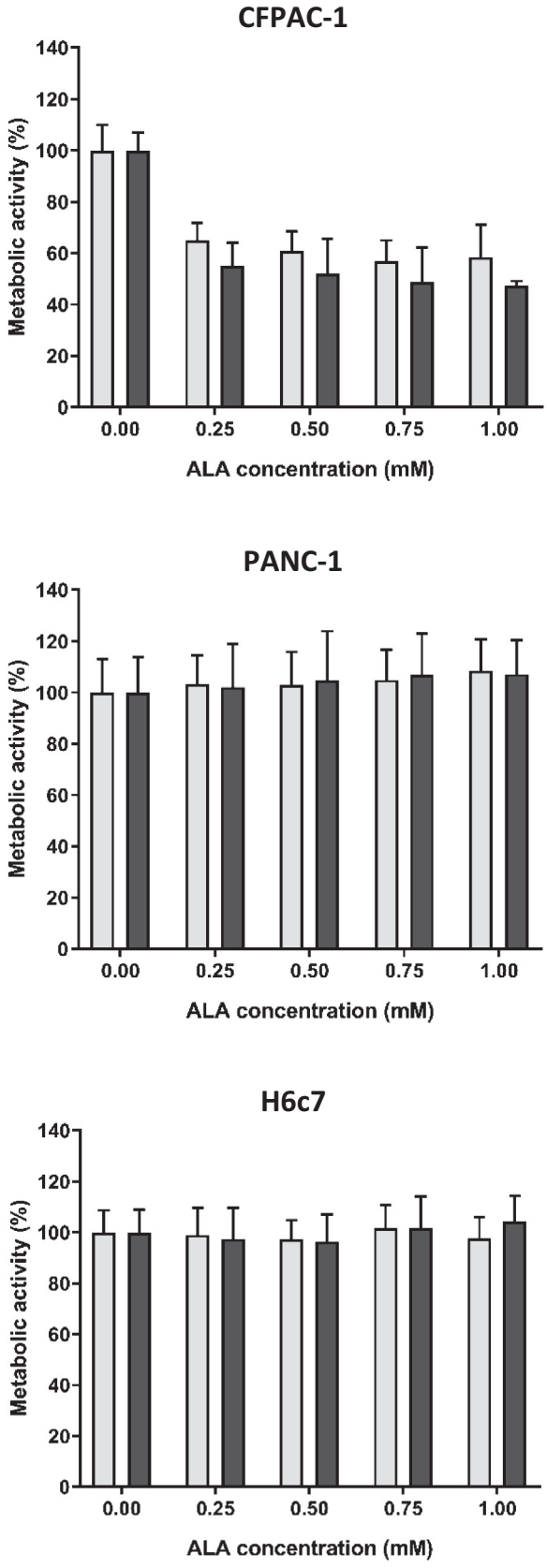

In vivo tumour-to-background ratios will almost certainly be lower than cell line SNRs as up to 90% of the tumour mass in pancreatic cancer consists of stromal cells such as cancer-associated fibroblasts, pancreatic stellate cells, endothelial cells and immune cells [21–23]. This is relevant because ALA has a predilection for epithelial and neoplastic cells over connective and non-neoplastic tissue such as stroma [24]. Animal models better represent the tumour microenvironment and could be used to develop systems to measure and enhance tumour-to-background ratios using ALA. For example, ALA was shown to generate a tumour-to-background ratio of ~5 in an allogenic hamster model using the hamster pancreatic cancer cell line PC-1 [25]. Genetically-engineered mouse models such as the KPC model could also assess the effect of ALA on pancreatic cancer precursor lesions as well as PDAC [26].

MTT assay showed no evidence of ALA toxicity in H6c7 and PANC-1, but significantly reduced metabolic activity in CFPAC-1 (Fig. 5). Given that cells appeared healthy on microscopy, MTT is reduced to formazan in the mitochondria [27], and mitochondria are the site of PpIX production, it is likely that ALA uptake caused a diversion of cell metabolism to PpIX formation resulting in reduced formazan production. Thus, the MTT result is unlikely to represent true cytotoxicity in CFPAC-1. Supporting this theory, flow cytometry showed that 85–90% of cells were alive in all samples in all cell lines, irrespective of the ALA content (data not shown). Unlike MTT, the flow cytometry viability dye is already fluorescent and enters dead cells through fenestrations in disrupted cell membranes. By only entering cells with membranous damage and fluorescing independently of cell metabolism, this circumvents the limitations of MTT assay in this context.

ALA is likely to enter CFPAC-1 via PEPT1 (Fig. 6). PDAC cell lines AsPC-1 and Capan-2 also express PEPT1 [28], and PEPT1 expression was more common in fluorescent tumours in the study by Yonemura et al. [13]. PEPT1 overexpression is associated with multiple malignancies including malignant glioma [29], bladder [30], stomach [31], bile duct [32], liver [33] and prostate cancer [34]. PEPT1 overexpression is associated with PpIX fluorescence in malignant glioma and ALA FGS is now recommended for glioma resection [10]. As PANC-1 was PEPT1 negative and showed negligible fluorescence following ALA exposure, these data support the notion that PEPT1 is the influx transporter for ALA in pancreatic cancer.

Several other variations in the haem biosynthesis pathway were identified. Decreased ALA synthase and increased ABCB6 transporter expression were common to all three cell lines following ALA exposure. PANC-1 and H6c7 also significantly upregulated porphyrin efflux transporter ABCG2. PEPT2, another ALA transporter [35], is expressed in H6c7 and may account for fluorescence seen in this cell line at higher concentrations. H6c7 up- or downregulated multiple enzymes and transporters following ALA exposure, fully suppressing the effect of 0.25 mM ALA. This may explain how non-cancerous tissues prevent intracellular PpIX accumulation compared to neoplastic tissues.

Several identified mechanisms could explain the negligible response to ALA in PANC-1. ALA influx transporters PEPT1 and PEPT2 were absent. ABCG2 was significantly upregulated following ALA exposure, which could prevent porphyrin accumulation. Other factors affecting ALA response not investigated in this study include mitochondrial function, cell-cycle stage, environmental factors (e.g. availability of iron) and the degree of cell differentiation [24]. Differentiating agents (e.g. vitamin D or methotrexate) increase PpIX production by upregulating coproporphyrinogen oxidase and downregulating ferrochelatase [7]. It is possible that low PpIX production in PANC-1 is secondary to poor differentiation, and treatment

Fig. 5. Cell metabolic activity of pancreatic cancer cell lines CFPAC-1 and PANC-1 and pancreatic ductal cell line H6c7 following 24 or 48 h dark incubation with increasing aminolevulinic acid concentration (MTT assay). ALA incubation for 24 or 48 h did not demonstrate any significant effect on cell metabolic activity in H6c7 or PANC-1 but caused a significant decrease in cell metabolic activity in CFPAC-1 at all investigated concentrations after 24 or 48 h (one-way ANOVA <0.001). Abbreviations: MTT = Methyl Thiazolyl Tetrazolium, ALA = aminolevulinic acid. Light grey = 24 h, dark grey = 48 h.

with a differentiating agent may enhance fluorescence. Vitamin D has been shown to increase PpIX accumulation in epidermoid skin cancer cell line A-431 and breast cancer cell line MDA-MB-231 [7,36]. This is yet to be investigated in PDAC.

Identifying PANC-1 as a PDAC cell line poorly responsive to ALA provides an easy in vitro experimental model to investigate drug therapies that aim to enhance PpIX accumulation in PDAC. ALA delivery via targeted nanocarriers may circumvent the issue of absent PEPT1 expression in PANC-1. This principle has been demonstrated in an orthotopic mouse model using the skin cancer cell line SCC-7 [37]. Other potential therapies include ferrochelatase inhibitors (e.g. iron chelators [38] or manganese chloride [39]) and ABCG2 inhibitors [40]. Differentiating agents such as vitamin D may be the easiest first step as they are already clinically available and are not expected to enhance uptake in normal pancreas as this should already be well differentiated.

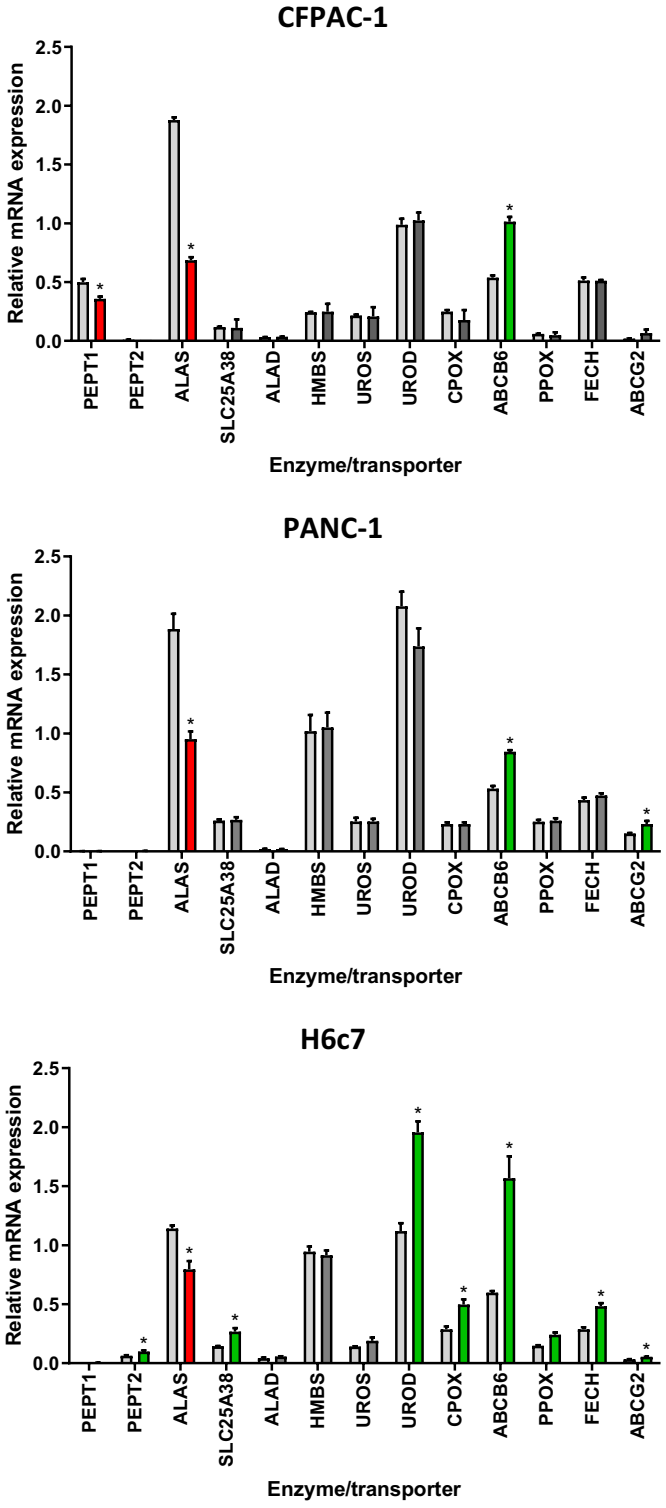

Fig. 6. Relative mRNA expression of enzymes and transporters involved in the haem biosynthesis pathway in pancreatic cancer cells lines CFPAC-1 and PANC-1 and pancreatic ductal cell line H6c7 with or without 24 h dark incubation with 0.5 mM aminolevulinic acid (expression normalised to HPRT1). First bar (light grey) = mRNA expression in the absence of ALA (control). Second bar = mRNA expression following 24 h incubation with 0.50 mM ALA (red = significant reduction in mRNA expression, green = significant increase in mRNA expression, dark grey = no significant increase or decrease in mRNA expression compared to control). *$p < 0.01$. Abbreviations: PEPT1/2 = Peptide Transporter 1/2, ALAS = ALA synthase, ALAD = ALA dehydratase, HMBS = hydroxymethylbilane synthase, UROS = uroporphyrinogen III synthase, UROD = uroporphyrinogen decarboxylase, CPOX = coproporphyrinogen oxidase, PPOX = protoporphyrinogen oxidase, FECH = ferrochelatase. (For interpretation of the references to colour in this figure legend, the reader is referred to the web version of this article.)

Focusing on clinical translation, it is already feasible to pre-operatively identify which patients have ALA-susceptible PDAC and may benefit from ALA FGS. Patients often undergo endoscopic ultrasound-guided fine needle aspiration (EUS-FNA) for tissue acquisition to confirm the diagnosis of PDAC prior to surgery. Ikeura et al. published a case series of 28 patients with pancreatic masses who were given ALA prior to EUS FNA [41]. Fluorescence cytology successfully identified all cancers ($n = 22$; 21 pancreatic) and benign diagnoses ($n = 6$), giving a sensitivity and specificity of 100%. Hirao and colleagues published a similar case series ($n = 53$) but incubated the EUS FNA samples in ALA ex vivo after acquisition [42]. All benign lesions were negative for fluorescence ($n = 7$) and 42/46 PDAC samples were positive for fluorescence, giving a sensitivity and specificity of 91.3% and 100% for fluorescence cytology compared to 93.5% and 85.7% for standard cytology. These studies show a dual effect of both improving the diagnostic accuracy of FNA cytology samples and identifying patients with ALA-susceptible PDAC who may benefit from ALA FGS. Identifying ALA as an effective contrast agent for FGS in PDAC also raises the possibility of exploiting its other recognised use as a photosensitiser for photodynamic therapy (PDT). In principle, ALA PDT could be used to treat the pancreatic bed in cases where small volume disease is still present but further resection is not possible. This could potentially reduce the risk of local recurrence, increasing the chance of cure.

Conclusion

This study identified factors that may explain variability in ALA-induced PpIX fluorescence between cancerous and non-cancerous pancreatic cells. Increasing ALA concentration is unlikely to improve contrast as the limiting factor is not the extracellular availability of ALA. Higher ALA concentrations increase fluorescence in non-neoplastic pancreatic ductal cells, leading to lower SNRs. Variations in ALA-induced PpIX fluorescence in PDAC may be related to PEPT1 and ABCG2 expression. PANC-1 could be used to investigate therapies to improve PpIX accumulation in PDAC with poor response to ALA.

Future studies should investigate the effects of vitamin D, ferrochelatase inhibitors and ABCG2 inhibitors on PDAC cell lines and H6c7 to determine the most effective drug combination to provide the highest SNRs. This combination should be assessed in an appropriate animal model to estimate the tumour-to-background ratio before advancing to early phase clinical trials. A study investigating PEPT1, PEPT2 and ABCG2 expression in patient-derived PDAC samples should be conducted to determine the proportion of pancreatic cancers that express these transporters.

CRediT authorship contribution statement

P.L. Labib: Conceptualization, Methodology, Formal analysis, Investigation, Writing - original draft, Visualization. **E. Yaghini:** Methodology, Writing - review & editing, Supervision. **B.R. Davidson:** Methodology,

Writing - review & editing, Supervision. **A.J. MacRobert:** Conceptualization, Methodology, Resources, Writing - review & editing, Supervision, Funding acquisition. **S.P. Pereira:** Conceptualization, Methodology, Resources, Writing - review & editing, Supervision, Funding acquisition.

Declaration of competing interest

The authors have no known competing financial interests or personal relationships that could have appeared to influence the work reported in this paper.

Acknowledgements

The authors thank Dr. Bala Ramesh, Ms. Shivajanani Sivakumaran-Nguyen and Dr. Walid Al-Akkad for assistance in microscopy, flow cytometry and qPCR protocol development. This work was supported in part by the UCLH/UCL Biomedical Research Centre which receives a proportion of funding from the Department of Health's National Institute for Health Research (NIHR) Biomedical Research Centres funding scheme.

References

[1] L. Huang, L. Jansen, Y. Balavarca, E. Molina-Montes, M. Babaei, L. van der Geest, et al., Resection of pancreatic cancer in Europe and USA: an international large-scale study highlighting large variations, Gut. 68 (1) (2019 Jan) 130–139.
[2] M. Kalisvaart, D. Broadhurst, F. Marcon, R. Pande, A. Schlegel, R. Sutcliffe, et al., Recurrence patterns of pancreatic cancer after pancreatoduodenectomy: systematic review and a single-centre retrospective study, HPB (Oxford) 22 (9) (Feb 2020) 1240–1249 S1365182X20300101.
[3] M.T. Olson, Q.P. Ly, A.M. Mohs, Fluorescence guidance in surgical oncology: challenges, opportunities, and translation, Mol. Imaging Biol. 21 (2) (2019 Apr) 200–218.
[4] J. Bushberg, J. Seibert, E. Leidholt Jr., J. Boone (Eds.), The Essential Physics of Medical Imaging, 3rd ed.Wolters Kluwer Health/Lippincott Williams & Wilkins, Philadelphia, 2012 , (1030 pp.).
[5] S. Hernot, L. van Manen, P. Debie, J.S.D. Mieog, A.L. Vahrmeijer, Latest developments in molecular tracers for fluorescence image-guided cancer surgery, Lancet Oncol. 20 (7) (2019 Jul) e354–e367.
[6] E. Suero Molina, S. Schipmann, W. Stummer, Maximizing safe resections: the roles of 5-aminolevulinic acid and intraoperative MR imaging in glioma surgery—review of the literature, Neurosurg. Rev. 42 (2) (2019 Jun) 197–208.
[7] X. Yang, P. Palasuberniam, D. Kraus, B. Chen, Aminolevulinic acid-based tumor detection and therapy: molecular mechanisms and strategies for enhancement, Int. J. Mol. Sci. 16 (10) (2015 Oct 28) 25865–25880.
[8] K. Omoto, R. Matsuda, Y. Nakai, Y. Tatsumi, T. Nakazawa, Y. Tanaka, et al., Expression of peptide transporter 1 has a positive correlation in protoporphyrin IX accumulation induced by 5-aminolevulinic acid with photodynamic detection of non-small cell lung cancer and metastatic brain tumor specimens originating from non-small cell lung cancer, Photodiagn. Photodyn. Ther. 25 (2019 Mar) 309–316.
[9] C. Hou, S. Yamaguchi, Y. Ishi, S. Terasaka, H. Kobayashi, H. Motegi, et al., Identification of PEPT2 as an important candidate molecule in 5-ALA-mediated fluorescence-guided surgery in WHO grade II/III gliomas, J. Neuro-Oncol. 143 (2) (2019 Jun) 197–206.
[10] National Institute for Health and Care Excellence (NICE), Brain tumours (primary) and brain metastases in adults [NICE guideline NG99], NICE, London, 2018.
[11] K. Orth, D. Russ, R. Steiner, H.G. Beger, Fluorescence detection of small gastrointestinal tumours: principles, technique, first clinical experience, Langenbeck's Arch. Surg. 385 (7) (2000 Nov 20) 488–494.
[12] T. Zöpf, A.R.J. Schneider, U. Weickert, J.F. Riemann, J.C. Arnold, Improved preoperative tumor staging by 5-aminolevulinic acid induced fluorescence laparoscopy, Gastrointest. Endosc. 62 (5) (2005 Nov) 763–767.
[13] Y. Yonemura, Y. Endo, E. Canbay, Y. Liu, H. Ishibashi, K. Takeshita, et al., Selection of patients by membrane transporter expressions for aminolevulinic acid (ALA)-guided photodynamic detection of peritoneal metastases, Int. J. Sci. 4 (9) (2015) 66–77.
[14] K. Harada, Y. Murayama, H. Kubo, H. Matsuo, R. Morimura, H. Ikoma, et al., Photodynamic diagnosis of peritoneal metastasis in human pancreatic cancer using 5-aminolevulinic acid during staging laparoscopy, Oncol. Lett. 16 (1) (2018) 821–828.
[15] E.L. Deer, J. González-Hernández, J.D. Coursen, J.E. Shea, J. Ngatia, C.L. Scaife, et al., Phenotype and genotype of pancreatic cancer cell lines, Pancreas 39 (4) (2010 May) 425–435.
[16] T. Furukawa, W.P. Duguid, L. Rosenberg, J. Viallet, D.A. Galloway, M.S. Tsao, Long-term culture and immortalization of epithelial cells from normal adult human pancreatic ducts transfected by the E6E7 gene of human papilloma virus 16, Am. J. Pathol. 148 (6) (1996 Jun) 1763–1770.
[17] H. Ouyang, L. Mou, C. Luk, N. Liu, J. Karaskova, J. Squire, et al., Immortal human pancreatic duct epithelial cell lines with near normal genotype and phenotype, Am. J. Pathol. 157 (5) (2000 Nov) 1623–1631.
[18] E. Rud, O. Gederaas, A. Høgset, K. Berg, 5-Aminolevulinic acid, but not 5-aminolevulinic acid esters, is transported into adenocarcinoma cells by system BETA transporters, Photochem. Photobiol. 71 (5) (2007 May 1) 640–647.
[19] M.M. Weir, D.I. Vernon, S.B. Brown, in: D.A. Cortese (Ed.), Influence of Serum Proteins on the Accumulation of Aminolaevulinic Acid-induced Protoporphyrin IX in Cells in Culture 1994, pp. 40–44 , Amelia Island, FL.
[20] B. Chen, Towards a personalized aminolevulinic acid (ALA)-based therapy (conference presentation), in: T. Hasan (Ed.), 17th International Photodynamic Association World Congress [Internet], SPIE, Cambridge, United States 2019, p. 8 , [cited 2020 Jul 25]. Available from: https://www.spiedigitallibrary.org/conference-proceedings-of-spie/11070/2526183/Towards-a-personalized-aminolevulinic-acid-ALA-based-therapy-Conference-Presentation/10.1117/12.2526183.full.
[21] G.S. Karagiannis, T. Poutahidis, S.E. Erdman, R. Kirsch, R.H. Riddell, E.P. Diamandis, Cancer-associated fibroblasts drive the progression of metastasis through both paracrine and mechanical pressure on cancer tissue, Mol. Cancer Res. 10 (11) (2012 Nov 1) 1403–1418.
[22] T. Murakami, Y. Hiroshima, R. Matsuyama, Y. Homma, R.M. Hoffman, I. Endo, Role of the tumor microenvironment in pancreatic cancer, Ann. Gastroenterol. Surg. 3 (2) (2019 Mar) 130–137.
[23] A. Vaziri-Gohar, M. Zarei, J.R. Brody, J.M. Winter, Metabolic dependencies in pancreatic cancer, Front. Oncol. 8 (2018 Dec 12) 617.
[24] A. Juzeniene, P. Mikolajewska, 5-aminolevulinic acid and its derivatives, in: M. Hamblin, Y. Huang (Eds.), Handbook of Photomedicine, CRC Press, London, 2014.
[25] J. Regula, B. Ravi, J. Bedwell, A. MacRobert, S. Bown, Photodynamic therapy using 5-aminolaevulinic acid for experimental pancreatic cancer – prolonged animal survival, Br. J. Cancer 70 (2) (1994 Aug) 248–254.
[26] K. Majumder, N. Arora, S. Modi, R. Chugh, A. Nomura, B. Giri, et al., A novel immunocompetent mouse model of pancreatic cancer with robust stroma: a valuable tool for preclinical evaluation of new therapies, J. Gastrointest. Surg. 20 (1) (2016 Jan) 53–65 (discussion 65).
[27] J. van Meerloo, G.J.L. Kaspers, J. Cloos, Cell sensitivity assays: The MTT assay, in: I.A. Cree (Ed.), Cancer Cell Culture [Internet], Humana Press, Totowa, NJ 2011, pp. 237–245 , [cited 2020 Jun 27]. (Methods in Molecular Biology; vol. 731). Available from: http://link.springer.com/10.1007/978-1-61779-080-5_20.
[28] D.E. Gonzalez, K.M. Covitz, W. Sadée, R.J. Mrsny, An oligopeptide transporter is expressed at high levels in the pancreatic carcinoma cell lines AsPc-1 and Capan-2, Cancer Res. 58 (3) (1998 Feb 1) 519–525.
[29] H. Stepp, W. Stummer, 5-ALA in the management of malignant glioma, Lasers Surg. Med. 50 (5) (2018 Jul) 399–419.
[30] Y. Hagiya, Y. Endo, Y. Yonemura, K. Takahashi, M. Ishizuka, F. Abe, et al., Pivotal roles of peptide transporter PEPT1 and ATP-binding cassette (ABC) transporter ABCG2 in 5-aminolevulinic acid (ALA)-based photocytotoxicity of gastric cancer cells in vitro, Photodiagn. Photodyn. Ther. 9 (3) (2012 Sep) 204–214.
[31] M. Inoue, T. Terada, M. Okuda, K.-I. Inui, Regulation of human peptide transporter 1 (PEPT1) in gastric cancer cells by anticancer drugs, Cancer Lett. 230 (1) (2005 Dec 8) 72–80.
[32] J. Neumann, M. Brandsch, δ-Aminolevulinic acid transport in cancer cells of the human extrahepatic biliary duct, J. Pharmacol. Exp. Ther. 305 (1) (2003 Apr 1) 219–224.
[33] Y. Gong, J. Zhang, X. Wu, T. Wang, J. Zhao, Z. Yao, et al., Specific expression of proton-coupled oligopeptide transporter 1 in primary hepatocarcinoma-a novel strategy for tumor-targeted therapy, Oncol. Lett. 14 (4) (2017 Oct) 4158–4166.
[34] W. Tai, Z. Chen, K. Cheng, Expression profile and functional activity of peptide transporters in prostate cancer cells, Mol. Pharm. 10 (2) (2013 Feb 4) 477–487.
[35] F. Döring, J. Walter, J. Will, M. Föcking, M. Boll, S. Amasheh, et al., Delta-aminolevulinic acid transport by intestinal and renal peptide transporters and its physiological and clinical implications, J. Clin. Invest. 101 (12) (1998 Jun 15) 2761–2767.
[36] K.R. Rollakanti, S. Anand, E.V. Maytin, Vitamin D enhances the efficacy of photodynamic therapy in a murine model of breast cancer, Cancer Med. 4 (5) (2015 May) 633–642.
[37] J. Wu, H. Han, Q. Jin, Z. Li, H. Li, J. Ji, Design and proof of programmed 5-aminolevulinic acid prodrug nanocarriers for targeted photodynamic cancer therapy, ACS Appl. Mater. Interfaces 9 (17) (2017 May 3) 14596–14605.
[38] P. Palasuberniam, D. Kraus, M. Mansi, A. Braun, R. Howley, K.A. Myers, et al., Ferrochelatase deficiency abrogated the enhancement of aminolevulinic acid-mediated protoporphyrin IX by iron chelator deferoxamine, Photochem. Photobiol. 95 (4) (2019 Mar 15) 1052–1059 php.13091.
[39] T. Amo, N. Kawanishi, M. Uchida, H. Fujita, E. Oyanagi, T. Utsumi, et al., Mechanism of cell death by 5-aminolevulinic acid-based photodynamic action and its enhancement by ferrochelatase inhibitors in human histiocytic lymphoma cell line U937, Cell Biochem. Funct. 27 (8) (2009 Dec) 503–515.
[40] H. Kobuchi, K. Moriya, T. Ogino, H. Fujita, K. Inoue, T. Shuin, et al., Mitochondrial localization of ABC transporter ABCG2 and its function in 5-aminolevulinic acid-mediated protoporphyrin IX accumulation, PLoS One 7 (11) (2012), e50082, .
[41] T. Ikeura, M. Takaoka, K. Uchida, M. Shimatani, H. Miyoshi, K. Kato, et al., Fluorescence cytology with 5-aminolevulinic acid in EUS-guided FNA as a method for differentiating between malignant and benign lesions (with video), Gastrointest. Endosc. 81 (6) (2015) 1457–1462.
[42] M. Hirao, A. Hosui, A. Mimura, T. Tanimoto, K. Ohnishi, Y. Kusumoto, et al., Significance of in vitro photodynamic cytodiagnosis using 5-aminolevulinic acid in solid pancreatic tumors extracted by endoscopic ultrasound-guided fine-needle aspiration, Photodiagn. Photodyn. Ther. 101581 (2019 Oct).